parallel sequencing with the HiSeq 2000 platform with 100 bp paired-end reads (Illumina, San Diego, CA, USA). Candidate germline variants were detected through our in-house pipeline for WES analysis with minor modifications for the detection of germline variants (Yoshida *et al*, 2011; Kunishima *et al*, 2013). The resultant sequences were aligned to the University of California Santa Cruz (UCSC) Genome Browser hg19 with the Burrows-Wheeler Aligner (Li & Durbin, 2009). After removal of duplicate artifacts caused by polymerase chain reaction (PCR), the single nucleotide variants with an allele frequency >0·25 and insertion-deletions with an allele frequency >0·1 were called. With a mean depth of coverage of 116·3× (67× – 166×), more than 92% of the 50 Mb target sequences were analysed by more than 10 independent reads.

Target deep sequencing analysis was performed for the RP genes with a low depth of coverage of <10×. Amplification of the genome was accomplished by long PCR reactions using KOD-FX-Neo DNA polymerase (TOYOBO, Osaka, Japan) using the primers described in Data S1. The PCR products were used for library preparation after determination of their quantity by the Qubit dsDNA HS Assay (Life Technologies, Invitrogen division, Darmstadt, Germany). Libraries were prepared using the Nextera XT DNA Sample Preparation Kit (Illumina) according to the manufacturer's recommendation. Sequencing reactions were carried out using the MiSeq v2 (2 × 150 bp) chemistries (Illumina). The MiSeq re-sequencing protocol for amplicon was performed. The sequences were mapped on the human GRCh37/hg19 assembly and quality-checked using the on-board software MiSeq Reporter, and analysed by AVADIS NGS software (Agilent Technologies).

To validate *RPL27* and *RPS27* mutations of patients and their families, we performed direct sequencing analysis using the primers described in Data S1.

Cell lines and transient transfection with small interfering RNA

The human erythroleukaemic cell line K562 was maintained in RPMI 1640 medium (Sigma-Aldrich, St. Louis, MO, USA) supplemented with 10% fetal bovine serum (FBS) (Life Technologies, Carlsbad, CA, USA) at 37°C in a 5% CO_2 atmosphere. To knock down the *RPL27* and *RPS27* genes, cells were transfected by using Amaxa Nucleofector (Amaxa Biosystems, Gaithersburg, MD, USA) (Nucleofector solution V, Nucleofector program T-16) with 5 μl of 40 nmol/l siRNA solutions per 2 × 10^6 cells. The siRNA purchased from Thermo-Fisher Scientific-Dharmacon (Waltham, MA, USA) were ON-TARGET plus SMART pool human *RPS19, RPL5, RPS27, RPL27* and a non-targeting pool.

Northern blot analysis

Total RNA was extracted from cells using the RNeasy plus kit (QIAGEN), and hybridized at high stringency. The probes used in the present study are described in Data S1.

Functional analysis using zebrafish

Morpholino antisense oligonucleotides (MOs) targeting zebrafish *rpl27* and *rps27*, orthologs of human *RPL27* and *RPS27* respectively, were obtained from Gene Tools, LLC (Philomath, OR, USA). They were injected at a concentration of 5·0 or 20 μg/μl into one-cell-stage embryos. The MO-injected embryos (morphants) were grown at 28·5°C. Haemoglobin staining was performed at 48 h post-fertilization (hpf) using *o*-dianisidine (Uechi *et al*, 2006; Torihara *et al*, 2011).

Full-length *rpl27* was amplified by PCR and cloned into a pCS2+ vector for *in vitro* transcription. Capped mRNAs were synthesized from the linearized template using an mMessage mMachine SP6 kit (Life Technologies) and injected at 250 ng/μl into one-cell-stage embryos.

Total RNA was isolated from wild-types and the morphants. Reverse transcription (RT)-PCR was used to distinguish normal or cryptic sizes of the *rpl27* and *rps27.1* transcripts. This was performed by using primer pairs designed at exons 1 and 5 and exons 1 and 4, respectively. The MO and primer sequences are described in Data S1.

Results

Whole exome-sequencing analysis

A total of 98 Japanese DBA patients were registered and blood genomic DNA samples were collected. All samples were first screened for mutations in eight of 10 known DBA genes (*RPL5, RPL11, RPL35A, RPS10, RPS17, RPS19, RPS24* and *RPS26*) as well as *RPS14*, which had been implicated in the 5q- myelodysplastic syndrome, a subtype of myelodysplastic syndrome characterized by a defect in erythroid differentiation (Ebert *et al*, 2008). Screening was achieved by direct sequence analysis accompanied by high-resolution melt analysis (HRM) (Konno *et al*, 2010). Among these patients, 38% (38/100) had identifiable DBA mutations (Table S1). Some of the patients were described in our previous reports (Konno *et al*, 2010; Kuramitsu *et al*, 2012). Then, we screened for large gene deletions in the remaining 60 patients using synchronized-quantitative-PCR DBA gene copy number assay and/or genome wide single nucleotide polymorphism array analysis (Kuramitsu *et al*, 2012). We found that 20% (12 of 60) of samples had large deletions in previously identified DBA genes (Table S1).

WES was performed on the remaining 48 patients who lacked documented mutations or large deletions involving known DBA genes by screening. We found gene alterations in *RPS7, RPS27, RPL3L, RPL6, RPL7L1, RPL8, RPL13, RPL14, RPL18A, RPL27, RPL31* and *RPL35A* in 12 patients, whose WES data have been deposited in the European Genome-phenome Archive (EGA) under accession number EGAS00001000875. WES failed to identify a single *GATA1* mutation (Table I). The substitution mutations observed in

Table I. Characteristics of patients investigated by whole-exome sequencing.

Patient (UPN)	Age at diagnosis	Gender	Inheritance	Abnormalities	Mutation
5	1 year	F	Sporadic	None	*RPL18A* c.481C>T p.Arg161Cys
7	1 month	M	Sporadic	SGA, craniofacial abnormalities, skin pigmentation	ND
13	3 months	F	Sporadic	None	ND
21	1 year	F	Familial	None	*RPS7* c.75+1G>A Splicing error, *RPL13* c.547C>T p.R183C
26	Birth	F	Sporadic	Spastic quadriplegia, congenital hip dislocation, severe myopia, optic nerve hypoplasia, growth retardation	ND
35	18 months	M	Familial	None	*RPL6* c.253_255del p.Lys85del
36 (35 cousin)	Birth	M	Familial	Hypospadias, cryptorchidism	ND (No *RPL6* mutation was detected.)
37	4 years	M	Sporadic	Hypospadias, cryptorchidism, SGA	ND
42	2 months	F	Sporadic	None	*RPS27* c.89delC, p.Tyr31Thrfs*5
48	NA	NA	Sporadic	Fetal hydrops	*RPL3L* c.76C>G p.Arg26Gly
49	2 months	M	Sporadic	SGA, growth retardation	ND
50	2 months	F	Familial	Neutropenia	ND
52 (50 sister)	6 months	F	Familial	Neutropenia	ND
51	7 months	F	Sporadic	None	ND
53	8 months	F	Sporadic	SGA	ND
54	8 years	F	Sporadic	None	ND
61	9 months	M	Sporadic	None	ND
67	3 years	M	Sporadic	None	ND
68	16 months	M	Sporadic	None	*RPL14* c.446CTG(9), c.446CTG(15)
69	1 year	M	Sporadic	Flat thenar	ND
75	Birth	F	Familial	Acetabular dysplasia, total anomalous pulmonary venous connection	ND
76	Birth	M	Sporadic	IgG subclass 2 and 4 deficiency	*RPL35A* c.125A>G:p.Tyr42Cys *RPL7L1* c.G544A:p.V182I (His unaffected parents did not possess the mutation in *RPL35A*.)
77	Birth	M	Familial	None	ND
83	9 months	M	Sporadic	None	*RPL31* c.122G>A p.Arg41His
88	Birth	M	Familial	Cryptorchidism, hypospadias, learning disabilities	ND
89 (88 father)	NA	M	Familial	Skeletal malformation of fingers, growth retardation	ND
90	10 months	M	Sporadic	None	ND
91	Birth	F	Sporadic	None	*RPL8* c.413C>T p.Ser138Phe
93	11 months	M	Sporadic	Leucoderma, syndactyly	ND
95	Birth	F	Sporadic	Atrial septal defect, pulmonary stenosis	*RPL27* c.-2-1G>A Splicing error
96	28 months	F	Sporadic	None	ND
97	4 years	F	Sporadic	Growth retardation	ND
105	Birth	M	Sporadic	Growth retardation	ND
109	9 months	F	Sporadic	None	ND

Table I. (*Continued*)

Patient (UPN)	Age at diagnosis	Gender	Inheritance	Abnormalities	Mutation
112	4 months	F	Sporadic	Pulmonary atresia, tricuspid atresia, ventricular septal defect, hypoplasia of right ventricle, polydactyly of thumb, cerebellar hypoplasia, low-set ear, mandibular retraction, growth retardation	ND
116	4 months	M	Sporadic	Flat thenar	ND
117	NA	F	Sporadic	NA	ND
121	2 months	F	Sporadic	Growth retardation	ND
135	1 year	M	Sporadic	Xanthogranuloma	ND
136	Birth	M	Sporadic	None	ND
140	Birth	F	Sporadic	SGA	ND
144	2 months	F	Sporadic	Neutropenia	*RPL35A* c.125A>G p.Tyr42Cys (Her unaffected parents did not possess the mutation in *RPL35A*.)
151	9 months	M	Unknown	None	*RPL35A* c.113A>G p.Glu38Gly (His unaffected father was also heterozygous for the allele.)
152	NA	NA	Sporadic	None	ND
153	17 months	M	Sporadic	None	ND
154	NA	NA	NA	NA	ND
158	3 months	M	Sporadic	Patent ductus arteriosus	ND
159	8 months	M	Sporadic	None	ND

UPN, unique patient number; NA, not available; M, male; F, female; ND, not detected; SGA, small for gestational age.

RPL35A (Patients 76, 144 and 151) had escaped detection by the HRM analysis in the first step screening but were found by WES analysis. The mutations were confirmed by direct sequencing analysis. We speculated that the sensitivity of the HRM screening was insufficient for detection of these particular mutations because the size of the PCR amplicon containing the mutations was too large for the screening. A single missense mutation (c.125A>G: p.Tyr42Cys) observed in two of the sporadic DBA cases, Patients 76 and 144, was predicted to be causative because the unaffected parents of the two patients did not possess the mutation, suggesting that the mutations were *de novo* (Table I). Furthermore, tyrosine at position 42 is highly conserved among species. On the other hand, the pathological significance of the *RPL35A* mutation (c.113A>G p.Glu38Gly) observed in Patient 151 remains unknown because glutamic acid at position 38 is not well-conserved and the patient's unaffected father was also heterozygous for the allele (Table I).

The two known DBA genes, *RPS7* and *RPL26*, were not included in the first screening. Consequently, WES identified a *RPS7* mutation in Patient 21 and confirmed the mutation by direct sequencing. The mutation was predicted to be causative because it seemed to induce a splicing error in the gene. Mutations identified in the eight patients, including *RPL18A* in Patient 5, *RPL13* in Patient 21, *RPL6* in Patient 35, *RPL3L* in Patient 48, *RPL14* in Patient 68, *RPL7L1T* in Patient 76, *RPL31* in Patient 83 and *RPL8* in Patient 91, were missense mutations or in-frame deletions. Almost all of the causative variants of RP genes observed in DBA are loss-of function mutations (Gazda *et al*, 2012). Whereas analyses by SIFT, PolyPhen-2, Mutation Taster and CONDEL predicted that some of these mutations would probably damage the structure and function of ribosomal proteins, the pathological effects of the above-mentioned mutations were uncertain (Table S2). The substitution mutation of *RPL13* observed in Patient 21 seemed to be non-pathological because the *RPS7* splicing error mutation was also identified in this patient. The missense mutation in *RPL7L1T* found in Patient 76 also seemed to be non-pathological, because the *de novo* *RPL35A* mutation was identified in this patient. The in-frame deletion of *RPL6* observed in Patient 35 with familial DBA also might be non-causative, because the mutation was not identified in his cousin, Patient 36 (Table I).

De novo *mutation in* RPL27 *and* RPS27

Next, we focused on novel loss-of function mutations in *RPL27* and *RPS27*, found in the screening. Almost all RP genes were sequenced with enough coverage for detecting germline mutations except for several RP genes (Table S3). Target deep sequencing analysis was performed for the RP genes with a low depth of coverage of <10× (Table S4 and

S5), and we confirmed that the mutations in *RPL27* and *RPS27* were the only ones found in these patients.

In Patient 95, we identified the substitution of c.-2-1G>A in the *RPL27* gene, a putative splicing error mutation (Fig 1A). To confirm the effect of the mutation, we performed RT-PCR analysis by using primers located on the first and third exons and total RNA derived from the patient's leucocytes. We found two transcripts in Patient 95: the full-length transcript and a shorter transcript lacking exon 2 by alternative splicing, a variant skipping exon 2, in which the translation initiation codon is located (Fig 1B,C). We performed a quantitative assessment of the levels of the full-length transcripts and the short transcripts, using the Experion automated electrophoresis system (Bio-Rad, Hercules, CA, USA). The calculated concentration of each product was 48·31 nmol/μl (7·49 ng/μl) and 31·69 nmol/μl (3·19 ng/μl), respectively. The results indicated that the extent of aberrant splicing accounted for about 40% of total *RPL27* transcripts in this patient. Patient 95 was a 2-year-old girl with no family history of anaemia, diagnosed with DBA at birth. She had an atrial septal defect and pulmonary stenosis. She responded to corticosteroid treatment and has been in remission for 2 years. Her clinical characteristics are presented in Table II. As she was thought to be sporadic type DBA, we examined the genotype of her parents. The direct sequencing analysis showed that the parents were homozygous for wild-type *RPL27* (Fig 1A). These results suggested the mutation observed in the patient was *de novo* and a probable pathogenic mutation of DBA.

In Patient 42, we found a single nucleotide deletion (c.90delC, p.Tyr31Thrfs*5) in the *RPS27* gene generating a premature stop codon by frameshift (Fig 1D). The patient was a 4-year-old girl with no family history of anaemia, diagnosed with DBA at 2 months of age. This patient had no abnormalities except for skin pigmentation, and responded to steroid treatment. Her clinical characteristics are presented in Table II. Her unaffected parents did not have the gene alteration observed in the patients (Fig 1D), indicating the mutation was *de novo*.

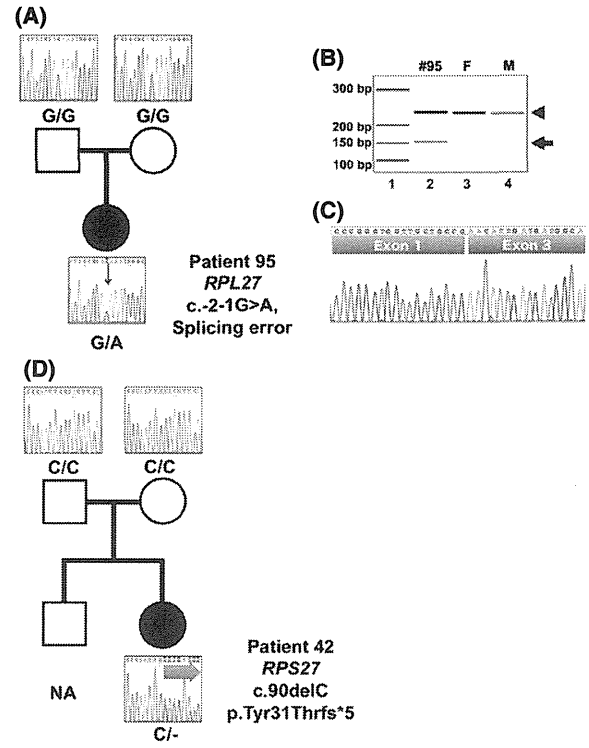

Fig 1. *De novo* mutations in *RPL27* and *RPS27*. (A) Family tree of Patient 95. Electropherograms indicate the gDNA sequence including the boundary between IVS-1 and the first exon of the *RPL27* gene. The red arrow indicates the position of the nucleotide substitution −2-1G>A observed in Patient 95. (B) RT-PCR analysis using the primer set located on the first and third exons of the *RPL27* gene. Arrowhead and arrow indicate PCR products for the full-length variant and the alternative splicing lacking the second exon, respectively. Molecular marker (lane 1), Patient 95 (lane 2), her father (F, lane 3) and mother (M, lane 4) are shown. (C) Sequence analysis of the short PCR product of Patient 95 showing the alternative splicing variants lacking the second exon. (D) Family tree of Patient 42. Electropherograms indicate gDNA sequence including a portion of the second exon of the *RPS27* gene. Blue arrow indicates the frameshift signals caused by single nucleotide deletion of c.90delC.

Defective pre-ribosomal RNA processing due to repression of RPL27 *or* RPS27

A single pre-ribosomal RNA (pre-rRNA), called 45S is processed into mature 28S, 18S and 5.8S rRNAs (Hadjiolova *et al*, 1993; Rouquette *et al*, 2005). Among the mature rRNAs, the 28S and 5.8S rRNAs associate with the large ribosomal subunit (60S) and the 18S rRNA associates with the small subunits (40S) of the ribosome. It has been reported that the mutations in RP genes observed in DBA cause defects in pre-rRNA processing. For example, the loss-of-function of the small subunit of RP affects maturation of 18S rRNA (Gazda *et al*, 2006, 2012; Choesmel *et al*, 2007; Flygare *et al*, 2007; Idol *et al*, 2007; Doherty *et al*, 2010). To validate the effects of the knockdown of *RPS27* or *RPL27* on erythroid lineage cells, we introduced siRNA into the human erythroid cell line K562 cells and analysed pre-rRNA processing by Northern blotting analysis.

Consistent with previous reports, decreased expression of *RPS19* was associated with a defect in rRNA processing characterized by a decrease in 18S-E rRNA with accumulation of a 21S rRNA precursor, and decreased expression of *RPS26* resulted in accumulation of a 26S rRNA precursor. Reduction of *RPS27* led to the accumulation of 30S rRNA and a decrease in the 21S rRNA and 18S-E rRNA (Fig 2). These findings suggest that RPS27 is also essential for 18S rRNA processing, although RPS27 involves rRNA processing associated with the small subunit at different stages from RPS19 and RPS26. In contrast, knockdown of *RPL27* caused accumulation of 32S rRNA, which is very similar to the effects by *RPL5* siRNA, suggesting that RPL27 is important for the

Table II. Clinical characteristics of DBA patients with *RPS27* or *RPL27* mutation.

UPN	42	95
Mutated gene	*RPS27*	*RPL27*
Age (years)	4	2
Gender	Female	Female
Family history of anaemia	No	No
Onset	2 months of age	At birth
Malformation	Skin pigmentation	Atrial septal defect pulmonary stenosis
Clinical data at onset		
RBC ($\times 10^{12}$/l)	1·38	2·17
Hb (g/l)	49	71
MCV (fl)	105	92·3
Reticulocytes (%)	0·17	0·1
WBC ($\times 10^{9}$/l)	11·68	5·5
Platelets ($\times 10^{9}$/l)	373	446
Bone marrow	Hyper cellularity, erythroid 1%	Normo-cellularity, erythroid 7·4%
Response to first steroid therapy	Yes	Yes
Present therapy	NA	NA

UPN, unique patient number; RBC, red blood cell count; WBC, white blood cell count; NA, not available.

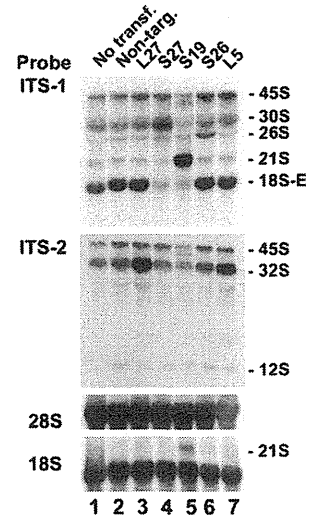

Fig 2. Perturbation of pre-rRNA processing by knockdown of the *RPL27* or *RPS27* gene. Northern blot analysis using K562 cells knocked down by siRNAs. The 5′ extremities of the internal transcribed spacer 1 (ITS-1) and internal transcribed spacer 2 (ITS-2) were used as probes to detect the precursors to the 18S rRNA associated with the small subunit and 28S rRNA and 5.8S rRNA associated with the large subunit of the ribosome, respectively. *RPS19, RPS26* and *RPL5* knocked-down cells were used as positive controls for the detection of defects in rRNA processing. ITS-1 and ITS-2 probes revealed the accumulation of 30S pre-rRNA in *RPS27* knocked-down cells and 32S pre-rRNA in *RPL27* knocked-down cells, respectively. Decrease of 18S-E pre-rRNA was also detected by the ITS-1 probe in *RPS27* knockdown cells. The mature 18S and 28S rRNAs were detected with specific probes.

maturation of 28S and 5.8S rRNAs (Fig 2). These findings showed that decreased expression of *RPS27* and *RPL27* perturbed pre-rRNA processing associated with the small and large subunits, respectively.

To accurately model the degree of ribosomal haploinsufficiency, we titrated the dose of the siRNA to obtain approximately 50% of the expression compared with wild-type cells (Figure S1A). For this experiment, we used 50% *RPS19, RPS26* and *RPL5* knocked-down cells as positive controls. However, the rRNA processing defects were not clearly observed under these conditions even in the positive controls (Figure S1B). These results suggested that a more accurate functional assay was necessary to investigate the pathological significance of these mutations. For that reason, we turned to the zebrafish model.

Impairment of erythroid development in rpl27 *and* rps27*-deficient zebrafish*

To investigate the effects of *RPL27* mutations in DBA, we knocked down the zebrafish ortholog (*rpl27*) using MOs and analysed the morphology and erythropoietic status during embryonic development. The coding region of *rpl27* shares 84% nucleotide and 96% amino acid identities with its human ortholog. Although gene duplication is common in zebrafish, available information from public databases suggests that *rpl27* exists as a single copy in the genome. We inhibited expression of this gene using an MO designed to target the 3′-splice site of the first intron that corresponded to the position at which the mutation was identified in the patient (Fig 3A). Injection of this MO into the one-cell stage embryos perturbed the splicing and resulted in exclusion of exon 2 as observed in the patient (Fig 3B). When injected with 5 μg/μl MO targeted against *rpl27*, the expression level of a smaller transcript lacking exon 2 was comparable to that seen in Patient 1 (Figs 1B and 3B). Therefore, all of the following experiments were performed using 5 μg/μl MO.

We compared the morphological features of the morphants with wild-type embryos and found that the morphants showed abnormal phenotypes, such as a thin yolk sac extension and a bent tail at 25 hpf (Fig 3C). We also performed haemoglobin staining at 48 hpf and found a marked reduction of erythrocyte production in the cardial vein of the morphants (Fig 3D). All these abnormalities were rescued by the simultaneous injection of *rpl27* mRNA into the embryos, indicating that the morphological defects and decreased erythropoiesis observed in the morphants were caused by the aberrant splicing of *rpl27* in zebrafish (Fig 3B,D). These results suggested that the splice site mutation identified in human *RPL27* could be responsible for the pathogenesis of DBA.

We next investigated the effects of *RPS27* mutations in DBA. Public databases suggest that there are three copies of the zebrafish *rps27* gene, *rps27.1*, *rps27.2* and *rps27.3*, whereas

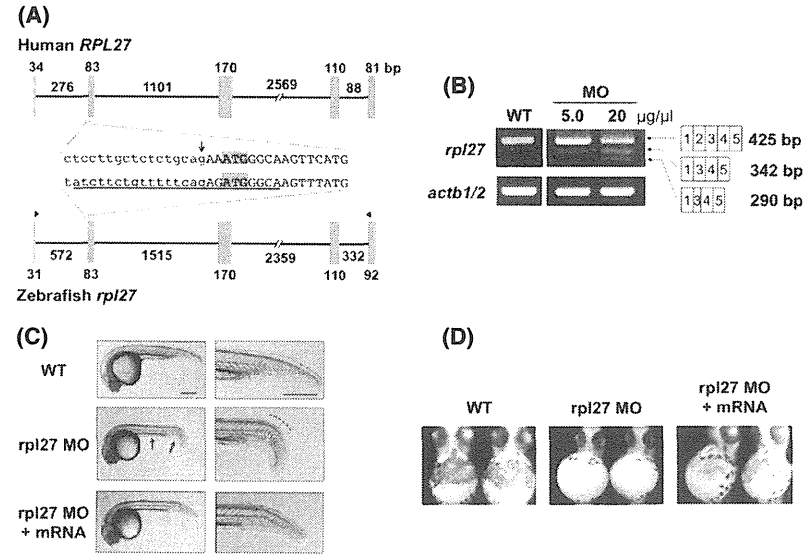

Fig 3. Morphological defects and decreased erythropoiesis in *rpl27* morphants. (A) The gene structures of human *RPL27* and zebrafish *rpl27*. The sequences of intron 1/exon 2 boundary regions are indicated. Uppercase and lowercase letters show the exon and intron sequences, respectively. The MO target site is underlined and the translation initiation codons (ATG) are shaded. The arrow indicates the position of the mutated nucleotide in the patient. Arrowheads show the primer positions for the RT-PCR. (B) The results of RT-PCR of *rpl27* and *actb* (control) in wild type and MO injected embryos. A smaller transcript without exon 2 was observed in the morphants as seen in the patient at a comparable level, when 5 μg/μl MO was injected into the one-cell-stage embryos. Injection with higher concentrations of MO (20 μg/μl) also produced a truncated exon 3. (C) Morphological features of wild-type and MO-injected embryos. A thin yolk sac extension and a bent tail are prominent in the morphants injected with 5 μg/μl MO (arrows), whereas these features are rescued in the embryos injected with *rpl27* mRNA. Scale bars: 250 μm. (D) The haemoglobin staining of cardial veins at 48 hpf. Compared to wild-type embryos, *rpl27* morphants injected with 5 μg/μl MO showed a drastic reduction in the number of haemoglobin-stained blood cells. Morphants co-injected with *rpl27* mRNA show recovery of the stained cells.

the human genome contains two copies, *RPS27* and *RPS27L*. We inhibited expression of the zebrafish *rps27.1*, which shares 96% amino acid identity with the human *RPS27*, using an MO designed to target the 5′-splice site of the second intron (Fig 4A). Injection of this MO into the embryos perturbed the splicing and resulted in exclusion of exon 2 (Fig 4B) that consequently introduced a stop codon in exon 3. The morphants showed abnormal phenotypes, such as a thin yolk sac extension, a bent tail and a malformed brain region at 26 hpf (Fig 4C). We also observed reduced erythrocyte production in about 60% of the morphants (Fig 4D). These results suggested that the frameshift mutation identified in human *RPS27* is a strong candidate for a causative mutation for DBA.

Discussion

WES analysis identified loss-of-function mutations in two RP genes. Each of the patients carrying one of these mutations was a sporadic case, and the mutations were *de novo*. Knockdown of *RPL27* and *RPS27* disturbed pre-rRNA processing for the large and small subunits, respectively. Although the zebrafish models cannot reproduce the exact features of DBA, such as macrocytic anaemia appearing after birth and skeletal abnormalities, the models of *RPL27* and *RPS27* mutations showed impairment of erythrocyte production. These results suggested that *RPL27* and *RPS27* play important roles in erythropoiesis, and that haploinsufficiency of either RP could lead to pure red cell aplasia. However, these findings only represent a single patient in relation to each gene. The identification of new DBA cases in the future with mutations in these genes will be important to confidently label *RPS27* and *RPL27* as DBA disease genes.

Interestingly, RPS27 binds to MDM2 through its N-terminal region, and overexpression of RPS27 stabilizes TP53 by inhibiting MDM2-induced TP53 ubiquitination (Xiong *et al*, 2011). Although the exact mechanism by which ribosome disruptions leads to DBA is unclear, a widely accepted hypothesis is that imbalances in expression of individual RPs trigger a TP53-mediated checkpoint, leading to cell cycle arrest and apoptosis of erythroid precursors (Narla & Ebert, 2010). Several animal models have demonstrated the role of TP53 in the pathophysiology of DBA (McGowan & Mason, 2011). In support of this conclusion, it was observed that certain RPs, such as RPL5, RPL11, RPL23, RPL26 and RPS7, bind to and inhibit the TP53 regulator MDM2, thereby inhibiting its ability to promote TP53 degradation (Zhang & Lu, 2009). Notably, like *RPL27*, many of the RP genes, including *RPL5*, *RPL11*, *RPL26* and *RPS7*, are mutated in DBA.

Here, we report the results of RP gene mutations observed in 98 Japanese DBA patients. The frequency of the patients harbouring probable causative mutations/large

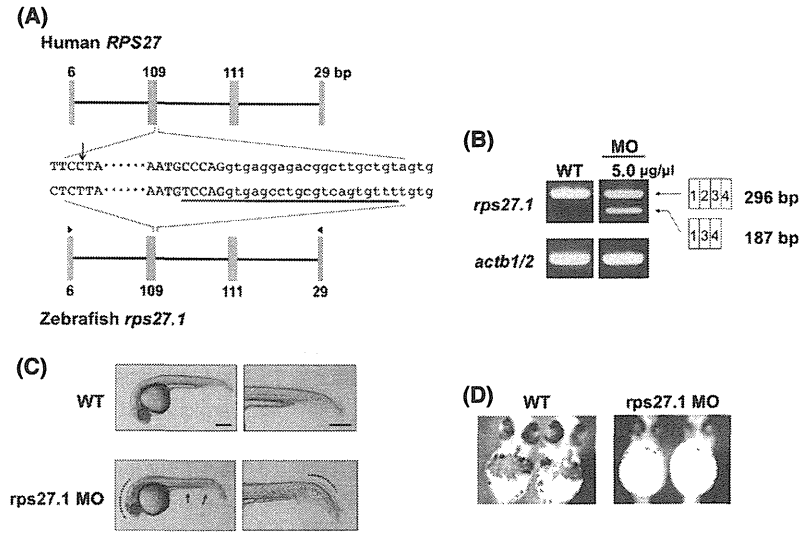

Fig 4. Morphological defects and decreased erythropoiesis in *rps27* morphants. (A) The gene structures of human *RPS27* and zebrafish *rps27.1*. The sequences of exon 2/intron 2 boundary regions are indicated. Uppercase and lowercase letters show the exon and intron sequences, respectively. The MO target site is underlined. The arrow indicates the position of the mutated nucleotide in the patient. Arrowheads show the primer positions for RT-PCR. (B) The results of RT-PCR of *rps27.1* and *actb* (control) in wild-type and MO-injected embryos. A smaller transcript without exon 2 was observed in the morphants. (C) Morphological features of wild-type and MO-injected embryos at 26 hpf. A thin yolk sac extension and a bent tail are prominent in the morphants (arrows). An abnormal development in the brain region was also observed. Scale bars: 250 μm. (D) Haemoglobin staining of cardial veins at 48 hpf.

deletions in RP genes was 55% (56/98), including *RPS19* 16% (16), *RPL5* 12% (12), *RPL11* 5% (5), *RPS17* 7% (7), *RPL35A* 7% (7), *RPS26* 4% (4), *RPS10* 1% (1), *RPS7* 1% (1), *RPL27* 1% (1) and *RPS27* 1% (1). No mutation of *RPS24*, *RPS29* or *RPL26* was identified in this study. In addition to above mutations, we found a missense mutation of *RPL35A* in a sporadic case (Patient 151). Mutations in RP genes are characterized by a wide variability of phenotypic expression. Even family members with the same mutation in the RP gene can present with clinical differences (Willig *et al*, 1999). For example, *RPS19* mutations are found in some first-degree relatives presenting only with isolated high erythrocyte adenosine deaminase activity and/or macrocytosis. Therefore, there is still the possibility that this *RPL35A* mutation is disease-causing, although the patients' father had the same heterozygous mutation without anaemia. To confirm the pathological effect of the substitution, a functional analysis is necessary. The zebrafish model might be very useful for this assay.

Recently, Gerrard *et al* (2013) found inactivating mutations in 15/17 patients by targeted sequencing of 80 RP genes. All mutations were in genes previously found to be DBA genes. The differences between these results and those in our study might be due to differences between human populations. In our cohort, all patients were Asian, whereas 80% were Caucasian in the cohort reported by Gerrard *et al* (2013). The frequency of RP gene mutaitons may vary between ethnic groups. However, the data from both cohorts are based on a relatively low number of patients and values showing significant differences between cohorts are missing. Interestingly, Gazda *et al* (2012) reported large-scale sequencing of 79 RP genes in a cohort of 96 DBA probands, none of whom had previously been found to have a pathogenic mutation. The study showed *c.* 53·9% of DBA patients had mutations in one of 10 known DBA-associated RP genes, including a novel causative *RPL26* gene. The results were very similar to ours, although their data did not contain large deletions of RP genes, which would escape regular sequencing analysis.

An additional five missense single nucleotide variants affecting single cases were identified in six patients, including *RPL3L*, *RPL7L1*, *RPL8*, *RPL13*, *RPL18A* and *RPL31* together with two in-frame deletions of *RPL6* and *RPL14* in two patients, which cause deletion of a single amino-acid (Table I). However, the pathological significance in these seven cases is uncertain. In the remaining 36 patients, no mutations were detected in *RP* genes. In conclusion, we identified novel germline mutations of two RP genes that could be responsible for DBA, further confirming the concept that RP genes are common targets of germline mutations in DBA patients and also suggesting the presence of non-RP gene targets for DBA. To identify the candidate disease variants in non-RP genes, we are now pursuing WES of their parents and planning to perform functional assays of these variants.

Acknowledgements

We thank T. Kudo and A. Mikami for their technical assistance. This work was supported by the Research on Measures for Intractable Diseases Project and Health and Labor

Sciences Research grants (Research on Intractable Diseases) from the Ministry of Health, Labour and Welfare, by Grants-in-Aid from the Ministry of Health, Labour and Welfare of Japan and by grants-in-aid for scientific research from the Ministry of Education, Culture, Sports, Science and Technology of Japan (KAKENHI: 25291003).

Authorship and Disclosure

Y.O., Y. S., A.S.-O., K.C., H.T. and S.M. performed bioinformatics analyses of the resequencing data. R.W., K.Y., T.T. and R.K. processed and analysed genetic material, prepared the library and performed sequencing. R.W., K.Y., T.T. and R.K. performed the Northern blot analyses and RT-PCR analyses. M.K and I.H. performed DBA copy number analysis. T. S., T. U. and N.K. performed zebrafish experiments. K. K., I.K., S. Ohga, A.O., J.H., K.S., K.M., K. K., A.I., Y. K., S.K., K.T., T. S. and E.I. collected specimens and were involved in planning the project. Y.I. and H.K. analysed data and designed the study. E.I. and S.O led the entire project. T.T., R.W., N.K. and I.E. wrote the manuscript. All authors participated in discussions and interpretation of the data and results.

Supporting Information

Additional Supporting Information may be found in the online version of this article:

Fig S1. Perturbation of pre-rRNA processing by knockdown of the *RPL27* or *RPS27* gene when the extent of the knockdown was approximately 50%.

Data S1. Methods.

Table S1. Mutations identified in *RPS19*, *RPL5*, *RPL11*, *RPL35A*, *RPS17* and *RPS26* in Japanese DBA patients.

Table S2. Prediction of functional effects of mutations in ribosomal protein genes.

Table S3. Mean coverage of whole-exome sequencing of RP genes in Patients #42 and #95.

Table S4. Average coverage of target deep sequencing of RP genes in Patient #95.

Table S5. Average coverage of target deep sequencing of RP genes in Patient #42.

References

Choesmel, V., Bacqueville, D., Rouquette, J., Noaillac-Depeyre, J., Fribourg, S., Crétien, A., Leblanc, T., Tchernia, G., Da Costa, L. & Gleizes, P.E. (2007) Impaired ribosome biogenesis in Diamond-Blackfan anemia. *Blood*, **109**, 1275–1283.

Cmejla, R., Cmejlova, J., Handrkova, H., Petrak, J. & Pospisilova, D. (2007) Ribosomal protein S17 gene (RPS17) is mutated in Diamond-Blackfan anemia. *Human Mutation*, **28**, 1178–1182.

Doherty, L., Sheen, M.R., Vlachos, A., Choesmel, V., O'Donohue, M.F., Clinton, C., Schneider, H.E., Sieff, C.A., Newburger, P.E., Ball, S.E., Niewiadomska, E., Matysiakm M, Glader., B., Arceci., R.J., Farrar., J.E., Atsidaftosm.E., Liptonm J, M., Gleizes, P.E. & Gazda, H.T. (2010) Ribosomal protein genes RPS10 and RPS26 are commonly mutated in Diamond-Blackfan anemia. *The American Journal of Human Genetics*, **86**, 222–228.

Draptchinskaia, N., Gustavsson, P., Andersson, B., Pettersson, M., Willig, T.N., Dianzani, I., Ball, S., Tchernia, G., Klar, J., Matsson, H., Tentler, D., Mohandas, N., Carlsson, B. & Dahl, N. (1999) The gene encoding ribosomal protein S19 is mutated in Diamond-Blackfan anaemia. *Nature Genetics*, **21**, 169–175.

Ebert, B.L., Pretz, J., Bosco, J., Chang, C.Y., Tamayo, P., Galili, N., Raza, A., Root, D.E., Attar, E., Ellis, S.R. & Golub, T.R. (2008) Identification of RPS14 as a 5q- syndrome gene by RNA interference screen. *Nature*, **451**, 335–339.

Farrar, J.E., Nater, M., Caywood, E., McDevitt, M.A., Kowalski, J., Takemoto, C.M., Talbot, C.C. Jr, Meltzer, P., Esposito, D., Beggs, A.H., Schneider, H.E., Grabowska, A., Ball, S.E., Niewiadomska, E., Sieff, C.A., Vlachos, A., Atsidaftos, E., Ellis, S.R., Lipton, J.M., Gazda, H.T. & Arceci, R.J. (2008) Abnormalities of the large ribosomal subunit protein, Rpl35a, in Diamond-Blackfan anemia. *Blood*, **112**, 1582–1592.

Flygare, J., Aspesi, A., Bailey, J.C., Miyake, K., Caffrey, J.M., Karlsson, S. & Ellis, S.R. (2007) Human RPS19, the gene mutated in Diamond-Blackfan anemia, encodes a ribosomal protein required for the maturation of 40S ribosomal subunits. *Blood*, **109**, 980–986.

Gazda, H.T., Grabowska, A., Merida-Long, L.B., Latawiec, E., Schneider, H.E., Lipton, J.M., Vlachos, A., Atsidaftos, E., Ball, S.E., Orfali, K.A., Niewiadomska, E., Da Costa, L., Tchernia, G., Niemeyer, C., Meerpohl, J.J., Stahl, J., Schratt, G., Glader, B., Backer, K., Wong, C., Nathan, D.G., Beggs, A.H. & Sieff, C.A. (2006) Ribosomal protein S24 gene is mutated in Diamond-Blackfan anemia. *The American Journal of Human Genetics*, **2006**, 1110–1118.

Gazda, H.T., Sheen, M.R., Vlachos, A., Choesmel, V., O'Donohue, M.F., Schneider, H., Darras, N., Hasman, C., Sieff, C.A., Newburger, P.E., Ball, S.E., Niewiadomska, E., Matysiak, M., Zaucha, J.M., Glader, B., Niemeyer, C., Meerpohl, J.J., Atsidaftos, E., Lipton, J.M., Gleizes, P.E. & Beggs, A.H. (2008) Ribosomal protein L5 and L11 mutations are associated with cleft palate and abnormal thumbs in Diamond-Blackfan anemia patients. *The American Journal of Human Genetics*, **83**, 769–780.

Gazda, H.T., Preti, M., Sheen, M.R., O'Donohue, M.F., Vlachos, A., Davies, S.M., Kattamis, A., Doherty, L., Landowski, M., Buros, C., Ghazvinian, R., Sieff, C.A., Newburger, P.E., Niewiadomska, E., Matysiak, M., Glader, B., Atsidaftos, E., Lipton, J.M., Gleizes, P.E. & Beggs, A.H. (2012) Frameshift mutation in p53 regulator RPL26 is associated with multiple physical abnormalities and a specific pre-ribosomal RNA processing defect in diamond-blackfan anemia. *Human Mutation*, **33**, 1037–1044.

Gerrard, G., Valgañón, M., Foong, H.E., Kasperaviciute, D., Iskander, D., Game, L., Müller, M., Aitman, T.J., Roberts, I., de la Fuente, J., Foroni, L. & Karadimitris, A. (2013) Target enrichment and high-throughput sequencing of 80 ribosomal protein genes to identify mutations associated with Diamond-Blackfan anaemia. *British Journal of Haematology*, **162**, 530–536.

Hadjiolova, K.V., Nicoloso, M., Mazan, S., Hadjiolov, A.A. & Bachellerie, J.P. (1993) Alternative pre-rRNA processing pathways in human cells and their alteration by cycloheximide inhibition of protein synthesis. *European Journal of Biochemistry*, **212**, 211–215.

Idol, R.A., Robledo, S., Du, H.Y., Crimmins, D.L., Wilson, D.B. & Ladenson, J.H. (2007) Cells depleted for RPS19, a protein associated with Diamond Blackfan anemia, show defects in 18S ribosomal RNA synthesis and small ribosomal subunit production. *Blood Cells Molecules and Diseases*, **39**, 35–43.

Ito, E., Konno, Y., Toki, T. & Terui, K. (2010) Molecular pathogenesis in Diamond-Blackfan anemia. *International Journal of Hematology*, **92**, 413–418.

Konno, Y., Toki, T., Tandai, S., Xu, G., Wang, R.N., Terui, K., Ohga, S., Hara, T., Hama, A., Kojima, S., Hasegawa, D., Kosaka, Y., Yanagisawa, R., Koike, K., Kanai, R., Imai, T., Hongo, T., Park, M.J., Sugita, K. & Ito, E. (2010) Mutations in the ribosomal protein genes in Japanese patients with Diamond-Blackfan anemia. *Haematologica*, **95**, 1293–1299.

Kunishima, S., Okuno, Y., Yoshida, K., Shiraishi, Y., Sandada, M., Muramatsu, H., Chiba, K., Tanaka, H., Miyazaki, K., Sakai, M., Ohtake, M., Kobayashi, R., Iguchi, A., Niimi, G., Otsu, M., Takahashi, Y., Miyano, S., Saito, H., Kojima, S. & Ogawa, S. (2013) ACTN1 mutations cause congenital macrothrombocytopenia. *The American Journal of Human Genetics*, **92**, 431–438.

Kuramitsu, M., Sato-Otsubo, A., Morio, T., Takagi, M., Toki, T., Terui, K., Wang, R., Kanno, H., Ohga, S., Ohara, A., Kojima, S., Kitoh, T., Goi, K., Kudo, K., Matsubayashi, T., Mizue, N., Ozeki, M., Masumi, A., Momose, H., Takizawa, K., Mizukami, T., Yamaguchi, K., Ogawa, S., Ito, E. & Hamaguchi, I. (2012) Extensive gene deletions in Japanese patients with Diamond-Blackfan anemia. *Blood*, **119**, 2376–2384.

Li, H. & Durbin, R. (2009) Fast and accurate short read alignment with Burrows-Wheeler transform. *Bioinformatics*, **25**, 1754–1760.

Lipton, J.M., Atsidaftos, E., Zyskind, I. & Vlachos, A. (2006) Improving clinical care and elucidating the pathophysiology of Diamond Blackfan anemia: an update from the Diamond Blackfan Anemia Registry. *Pediatric Blood & Cancer*, **46**, 558–564.

McGowan, K.A. & Mason, P.J. (2011) Animal models of Diamond Blackfan anemia. *Seminars in Hematology*, **48**, 106–116.

Mirabello, L., Macari, E.R., Jessop, L., Ellis, S.R., Myers, T., Giri, N., Taylor, A.M., McGrath, K.E., Humphries, J.M., Ballew, B.J., Yeager, M., Boland, J.F., He, J., Hicks, B.D., Burdett, L., Alter, B.P., Zon, L. & Savage, S.A. (2014) Whole-exome sequencing and functional studies identify RPS29 as a novel gene mutated in multi-case Diamond-Blackfan anemia families. *Blood*, **124**, 24–32.

Narla, A. & Ebert, B.J. (2010) Ribosomepathies: human disorders of ribosome dysfunction. *Blood*, **115**, 3196–3205.

Rouquette, J., Choesmel, V. & Gleizes, P.E. (2005) Nuclear export and cytoplasmic processing of precursors to the 40S ribosomal subunits in mammalian cells. *EMBO Journal*, **24**, 2862–2872.

Sankaran, V.G., Ghazvinian, R., Do, R., Thiru, P., Vergilio, J.A., Beggs, A.H., Sieff, C.A., Orkin, S.H., Nathan, D.G., Lander, E.S. & Gazda, H.T. (2012) Exome sequencing identifies *GATA1* mutations resulting Diamond-Blackfan anemia. *The Journal of Clinical Investigation*, **122**, 2439–2443.

Torihara, H., Uechi, T., Chakraborty, A., Shinya, M., Sakai, N. & Kenmochi, N. (2011) Erythropoiesis failure due to RPS19 deficiency is independent of an activated Tp53 response in a zebrafish model of Diamond-Blackfan anaemia. *British Journal of Haematology*, **152**, 648–654.

Uechi, T., Nakajima, Y., Nakao, A., Torihara, H., Chakraborty, A., Inoue, K. & Kenmochi, N. (2006) Ribosomal protein gene knockdown causes developmental defects in zebrafish. *PLoS ONE*, **1**, e37.

Vlachos, A., Ball, S., Dahl, N., Alter, B.P., Sheth, S., Ramenghi, U., Meerpohl, J., Karlsson, S., Liu, J.M., Leblanc, T., Paley, C., Kang, E.M., Leder, E.J., Atsidaftos, E., Shimamura, A., Bessler, M., Glader, B. & Lipton, J.M. (2008) Diagnosing and treating Diamond Blackfan anaemia: results of an international clinical consensus conference. *British Journal of Haematology*, **142**, 859–876.

Vlachos, A., Rosenberg, P.S., Atsidaftos, E., Alter, B.P. & Lipton, J.M. (2012) Incidence of neoplasia in Diamond Blackfan anemia: a report from the Diamond Blackfan Anemia Registry. *Blood*, **119**, 3815–3819.

Willig, T.N., Draptchinskaia, N., Dianzani, I., Ball, S., Niemeyer, C., Ramenghi, U., Orfali, K., Gustavsson, P., Garelli, E., Brusco, A., Tiemann, C., Pérignon, J.L., Bouchier, C., Cicchiello, L., Dahl, N., Mohandas, N. & Tchernia, G. (1999) Mutations in ribosomal protein S19 gene and diamond blackfan anemia: wide variations in phenotypic expression. *Blood*, **94**, 4294–4306.

Xiong, X., Zhao, Y., He, H. & Sun, Y. (2011) Ribosomal protein S27-like and S27 interplay with p53-MDM2 axis as a target, a substrate and a regulator. *Oncogene*, **30**, 1798–1811.

Yoshida, K., Sanada, M., Shiraishi, Y., Nowak, D., Nagata, Y., Yamamoto, R., Sato, Y., Sato-Otsubo, A., Kon, A., Nagasaki, M., Chalkidis, G., Suzuki, Y., Shiosaka, M., Kawahata, R., Yamaguchi, T., Otsu, M., Obara, N., Sakata-Yanagimoto, M., Ishiyama, K., Mori, H., Nolte, F., Hofmann, W.K., Miyawaki, S., Sugano, S., Haferlach, C., Koeffler, H.P., Shih, L.Y., Haferlach, T., Chiba, S., Nakauchi, H., Miyano, S. & Ogawa, S. (2011) Frequent pathway mutations of splicing machinery in myelodysplasia. *Nature*, **478**, 64–69.

Zhang, Y. & Lu, H. (2009) Signaling to p53: ribosomal proteins find their way. *Cancer Cell*, **16**, 369–377.

STEM CELLS TRANSLATIONAL MEDICINE

PLURIPOTENT STEM CELLS

Pluripotent Cell Models of Fanconi Anemia Identify the Early Pathological Defect in Human Hemoangiogenic Progenitors

NAOYA M. SUZUKI,[a] AKIRA NIWA,[a] MIHARU YABE,[b] ASUKA HIRA,[c] CHIHIRO OKADA,[d,e] NAOKI AMANO,[d] AKIRA WATANABE,[d] KEN-ICHIRO WATANABE,[f,g] TOSHIO HEIKE,[f] MINORU TAKATA,[c] TATSUTOSHI NAKAHATA,[a] MEGUMU K. SAITO[a]

Key Words. Induced pluripotent stem cells • Fanconi anemia • Hematopoietic progenitors • Differentiation • Transcription factors

Departments of [a]Clinical Application and [d]Reprogramming Science, Center for Induced Pluripotent Stem Cell Research and Application, and [c]Laboratory of DNA Damage Signaling, Department of Late Effects Studies, Radiation Biology Center, Kyoto University, Kyoto, Japan; [b]Department of Cell Transplantation and Regenerative Medicine, Tokai University School of Medicine, Isehara, Japan; [e]Mitsubishi Space Software Co., Ltd., Amagasaki, Japan; [f]Department of Pediatrics, Kyoto University Graduate School of Medicine, Kyoto, Japan; [g]Department of Hematology and Oncology, Shizuoka Children's Hospital, Shizuoka, Japan

Correspondence: Megumu K. Saito, M.D., Ph.D., 53 Shogoin-Kawahara-cho, Sakyo-ku, Kyoto 606-8507, Japan. Telephone: 81-75-366-7089; E-Mail: msaito@cira.kyoto-u.ac.jp

Received September 20, 2014; accepted for publication January 7, 2015.

1066-5099/2015/$20.00/0

http://dx.doi.org/10.5966/sctm.2013-0172

ABSTRACT

Fanconi anemia (FA) is a disorder of genomic instability characterized by progressive bone marrow failure (BMF), developmental abnormalities, and an increased susceptibility to cancer. Although various consequences in hematopoietic stem/progenitor cells have been attributed to FA-BMF, the quest to identify the initial pathological event is still ongoing. To address this issue, we established induced pluripotent stem cells (iPSCs) from fibroblasts of six patients with FA and *FANCA* mutations. An improved reprogramming method yielded iPSC-like colonies from all patients, and iPSC clones were propagated from two patients. Quantitative evaluation of the differentiation ability demonstrated that the differentiation propensity toward the hematopoietic and endothelial lineages is already defective in early hemoangiogenic progenitors. The expression levels of critical transcription factors were significantly downregulated in these progenitors. These data indicate that the hematopoietic consequences in FA patients originate from the early hematopoietic stage and highlight the potential usefulness of iPSC technology for elucidating the pathogenesis of FA-BMF. STEM CELLS TRANSLATIONAL MEDICINE *2015;4:1–6*

INTRODUCTION

Fanconi anemia (FA) is a disorder of genomic instability characterized by progressive bone marrow failure (BMF), developmental abnormalities, and an increased susceptibility to cancer [1–3]. The responsible genes form a common DNA repair network referred to as the FA pathway [4]. The FA pathway has been considered to be involved in repair of DNA interstrand cross-links (ICLs) [1–4]. The FA pathway is activated by ICL damage, leading to the monoubiquitination of Fanconi anemia, complementation group D2 (FANCD2) and Fanconi anemia, complementation group I (FANCI) proteins (ID complex) by FA core E3 ligase complex. The monoubiquitinated ID complex is then loaded on damaged chromatin and mediates homologous recombination and translesion synthesis. Although accelerated apoptosis and cell cycle arrest in hematopoietic stem/progenitor cells have been associated with BMF in patients with FA [5], precisely how and when the initial event that causes this consequence occurs have been unclear. Recent reports have indicated that the fate of hematopoietic progenitors has already been determined during fetal liver hematopoiesis both in humans and in mouse models of FA [5, 6]. However, tracing the earlier developmental events to capture the initial event is both technically and ethically impossible at present in humans.

Induced pluripotent stem cells (iPSCs) established from patients with FA may be useful to address these issues because, in combination with a proper hematopoietic differentiation system, iPSCs can enable evaluation of the human developmental stages [7, 8]. In this study, we established iPSCs from patients with FA and found that their differentiation propensity toward the hematopoietic lineage was already defective in the early hemoangiogenic progenitor stage. This report shows the possibility that the hematopoietic consequences in patients with FA originate at the earliest hematopoietic stage.

MATERIALS AND METHODS

Detailed methods are included in the supplemental online data.

Study Ethics

This study was approved by the ethics committees of Kyoto University and Tokai University, and informed consent was obtained from the

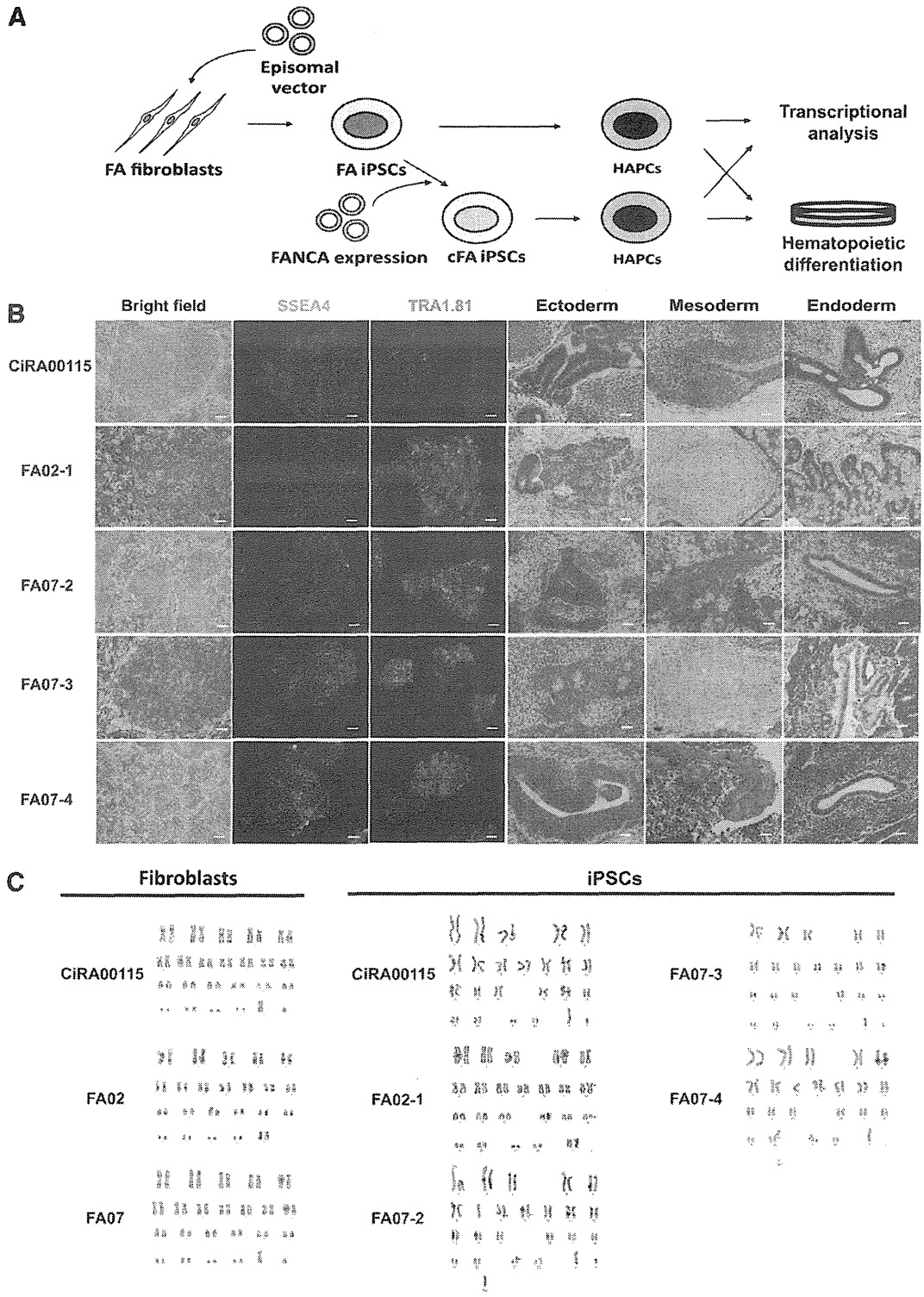

Figure 1. Establishment of FA-iPSC lines from patients with FA and mutations in *FANCA*. CiRA00115 is a control iPSC line. **(A):** The experimental scheme. **(B):** The morphology and immunostaining of pluripotent markers of FA-iPSCs and teratoma formation by the FA-iPSC lines (ectoderm: neural rosette; mesoderm: cartilage; endoderm: gut-like structure). Scale bars indicate 100 μm. **(C):** The results of karyotype analysis of fibroblasts and iPSCs from FA patients. The karyotypes of the fibroblasts were 46XX and 46XY for FA02 and FA07, respectively. The karyotype of FA-iPSCs from FA02 was summarized as 46, XX, t(12;18)(p11.2;p11.2) [20 cells]. The karyotypes of FA-iPSCs from FA07 were as follows: for FA07-2, 46, XY, add(1)(q32) [14 cells] and 46, XY [6 cells]; for FA07-3, 42-46, XY, add(8)(q24.1),add(11)(q23),del(11)(q23),add(18)(q21) [17 cells] and 42-46, XY, add(8)(q24.1),add(9)(q34),add(21)(p11.2) [3 cells]; for FA07-4, 45-46, XY, add(8)(q24.1),add(9)(q34),add(21)(p11.2) [20 cells]. Twenty metaphases were analyzed for each sample. Abbreviations: cFA, FANCA-complemented FA-iPSC clone; FA, Fanconi anemia; HAPC, hemoangiogenic progenitor cell; iPSC, induced pluripotent stem cell.

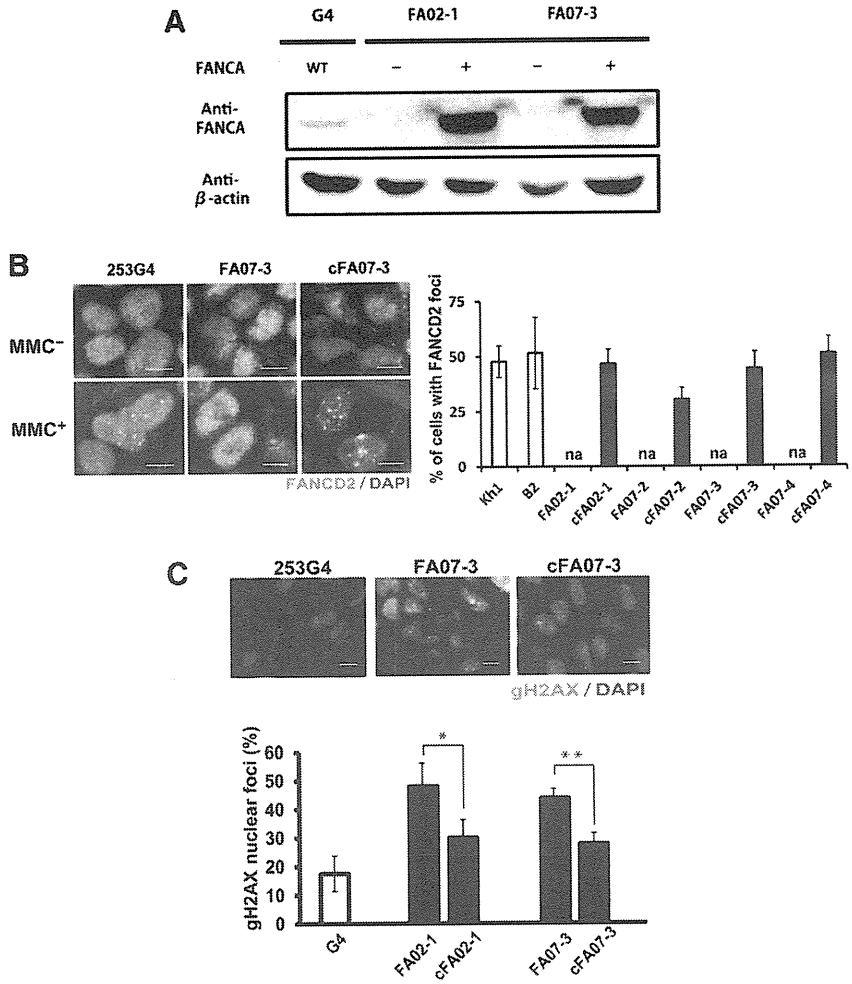

Figure 2. Validation of FA pathway in FA-iPSC lines. KhES1 is a control embryonic stem cell line, and 409B2 and 253G4 are control iPSC lines. **(A):** Immunoblotting for FANCA. **(B):** The formation of FANCD2 foci (green) in the nuclei (stained with DAPI; blue) of mitomycin C-treated FA-iPSCs (FA07) and cFA-iPSCs (cFA07) (left). The percentage of nuclei positive for FANCD2 foci (right). **(C):** Representative immunofluorescent staining (upper) and quantification (lower) of the nuclear foci of phosphorylated H2AX. The *y*-axis in the graph indicates the percentage of cells with three or more nuclear phosphorylated H2AX foci. All data are presented as mean ± SD and are representative of three independent experiments. All *p* values were determined by Student's *t* test. *, $p < .05$; **, $p < .01$ ($n = 3$). Scale bars indicate 10 μm. Abbreviations: cFA, FANCA-complemented FA-iPSC clone; DAPI, 4′, 6-diamidino-2-phenylindole; FA, Faconi anemia; iPSC, induced pluripotent stem cell; MMC, mitomycin C; WT, wild type.

patients' guardians in accordance with the Declaration of Helsinki.

Establishment and Differentiation of iPSCs From Patients With FA

Fibroblasts obtained from the six patients with FA (detail shown in supplemental online Table 1) were reprogrammed with episomal vectors encoding *OCT3/4, SOX2, KLF4, LIN28,* and *L-MYC* and a short hairpin RNA (shRNA) encoding a p53 knockdown sequence, as described previously [9]. Plasmids were kindly provided by Dr. Keisuke Okita (Kyoto University). For hematopoietic differentiation, a two-dimensional hematopoietic differentiation system was used, as described previously [10, 11].

Results and Discussion

We tried to reprogram fibroblasts obtained from six patients with FA and mutations in complementation group A (FA-A; patients with mutations in the Fanconi anemia, complementation group A [*FANCA*] gene) (supplemental online Table 1) by introducing the previously described reprogramming factors (*OCT3/4, SOX2, KLF4, c-MYC*) with retroviral [7] or Sendai viral vectors [12] under hypoxic conditions (5% O_2). Consistent with the previous reports [13], no iPSC-like colonies emerged. Recently, several groups reported that using a combination of highly efficient methods, including improved vectors such as a polycistronic OSKM cassette or additional reprograming factors under hypoxic culture conditions, could overcome the reprogramming resistance of FA cells [14–16]. Hence, we tried to establish FA patient-specific iPSCs by using episomal vectors encoding *OCT3/4, SOX2, KLF4, LMYC, LIN28,* and an shRNA-mediated p53 knockdown construct [9] under hypoxic conditions (5% O_2). As a result, iPSC-like colonies arose from all FA patient-derived fibroblasts (supplemental online Table 1); however, we could pick up and maintain only the TKFA02 and TKFA07 patient-derived iPSC (FA-iPSC) lines. The colonies arising from the TKFA03, FA44, FA45, and FA46 patients could not be picked up and propagated.

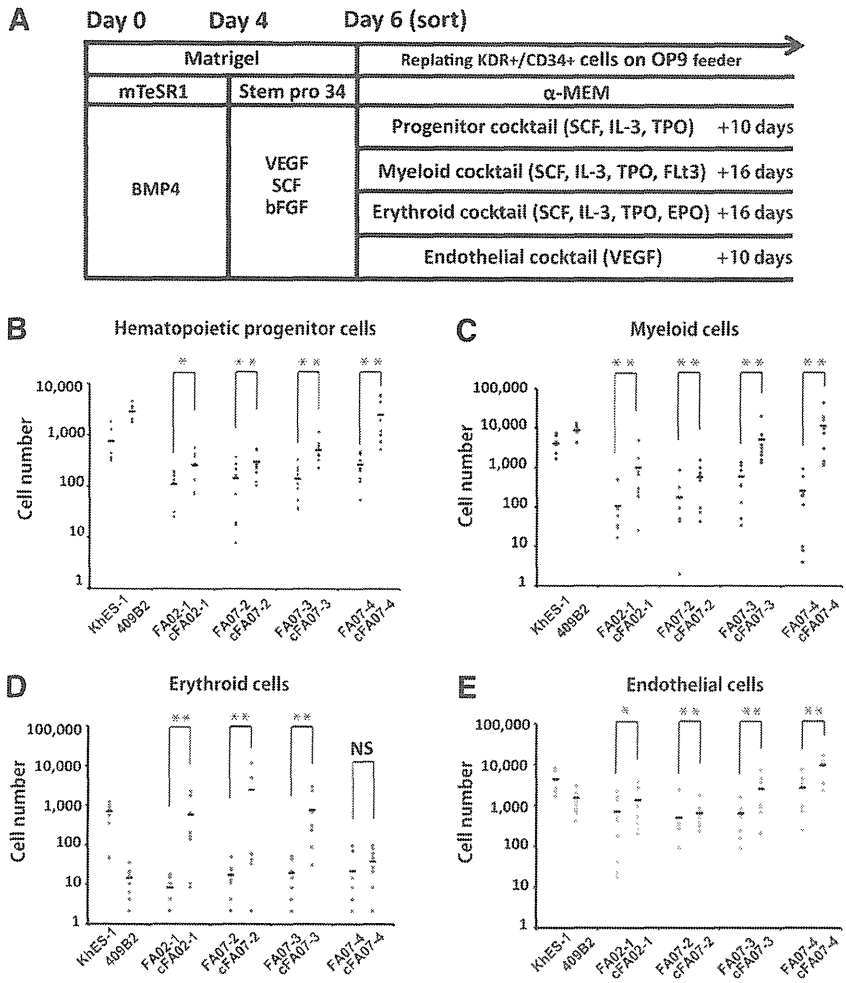

Figure 3. The defective differentiation propensity in Fanconi anemia induced pluripotent stem cell-derived hemoangiogenic progenitors. KhES1 and 409B2 are control embryonic and induced pluripotent stem cell lines, respectively. **(A):** A schematic diagram of hematopoietic differentiation. **(B–E):** The number of differentiated cells derived from 5,000 sorted KDR^+CD34^+ cells. **(B):** $CD34^+CD45^+$ hematopoietic progenitors. **(C):** $CD33^+CD45^+$ myeloid cells. **(D):** $CD45^-CD235\alpha^+$ erythroid cells. **(E):** $CD31^+CD34^+$ endothelial cells. All data are presented as mean ± SD and are representative of three independent experiments. All p values were determined by Wilcoxon rank sum test. *, $p < .05$; **, $p < .01$; ***, $p < .001$ ($n = 3$). Abbreviations: α-MEM, alpha Minimum Essential Medium; bFGF, basic fibroblast growth factor; EPO, erythropoietin; IL-3, interleukin 3; NS, not significant; SCF, stem cell factor; TPO, thyroid peroxidase; VEGF, vascular endothelial growth factor.

Consequently, we selected one and three FA-iPSC lines of the TKFA02 and TKFA07 cells, respectively (Fig. 1A).

The FA-iPSC lines showed human pluripotent cell-like morphology, expressed pluripotent markers, and differentiated into three germ layers in the teratoma formation assay (Fig. 1B). A short tandem repeated analysis confirmed that the patient identity was conserved throughout the reprogramming process (supplemental online Fig. 1). The FA-iPSC lines had residual transgene expressions, as reported previously [16] (supplemental online Fig. 2A). Consistent with this, these FA-iPSC clones, including their complemented counterparts (discussed below), showed reduced p53 expression (supplemental online Fig. 2B). Although the fibroblasts from both patients had normal karyotypes, both FA-iPSC lines had aberrant karyotypes (Fig. 1C), which is compatible with a previous report [16] and indicates that the FA pathway has an important role in determining chromosomal stability through reprogramming events. Collectively, by combining the reprogramming factors with modulation of the p53 pathway, we were able to develop a robust reprogramming strategy that enabled us to establish iPSC-like colonies from FA patient-derived somatic cells.

To establish isogenic FANCA-complemented clones, we introduced exogenous wild-type FANCA cDNA into each clone (Fig. 2A; supplemental online Fig. 3). Mitomycin C-induced FANCD2 foci formation was restored in these FANCA-complemented FA-iPSC clones (designated as cFA-iPSCs) (Fig. 2B). During maintenance of the iPSCs, the FA-iPSCs showed an increased DNA double-strand break rate, as evaluated by the frequency of nuclear foci of phosphorylated H2AX compared with the complemented counterparts (Fig. 2C), but the distribution of the cells in the different phases of the cell cycle was not significantly different (supplemental online Fig. 4). Consequently, the complementation of the FA pathway recovers the in vitro phenotype of FA-iPSCs.

To determine whether the hematopoietic differentiation is affected by disruption of the FA pathway, we next differentiated

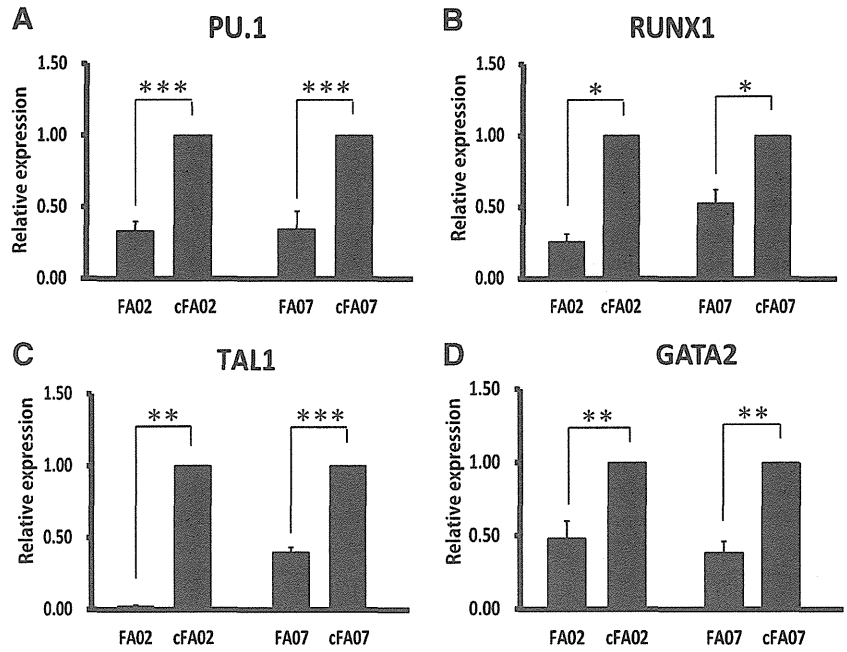

Figure 4. FANCA-deficient hemoangiogenic progenitor cells show the decreased expression of hematopoietic marker genes. **(A–D):** The results of the quantitative polymerase chain reaction analysis for hematopoietic marker genes in KDR^+CD34^+ hemoangiogenic progenitors (day 6). The relative gene expression (*y*-axis) was calculated relative to the expression in corresponding cFA induced pluripotent stem cells after normalization to the expression of glyceraldehyde-3-phosphate dehydrogenase. All data are presented as mean ± SD and are representative of three independent experiments. All *p* values were determined by Student's *t* test. *, $p < .05$; **, $p < .01$; ***, $p < .001$ ($n = 3$). Abbreviation: cFA, FANCA-complemented Fanconi anemia induced pluripotent stem cell clone.

the FA-iPSC lines into hematopoietic progenitor cells through the previously reported serum- and feeder-free monolayer culture system [10, 11]. Under this protocol, the progenitor cells committed to the hematopoietic lineage are obtained as KDR^+CD34^+ early hemoangiogenic progenitor cells (HAPCs), which give rise to both endothelial and hematopoietic cells. To evaluate the differentiation propensity of HAPCs quantitatively, we sorted the KDR^+CD34^+ HAPCs on day 6 and cultured them on OP9 feeder cells with lineage-specific cytokine cocktails (Fig. 3A; supplemental online Fig. 5). The FA-iPSC lines showed a significant reduction of $CD34^+CD45^+$ hematopoietic precursors compared with cFA-iPSC lines (Fig. 3B). Subsequently, the myeloid and erythroid lineage hematopoietic cells were significantly reduced (Fig. 3C, 3D). The number of $CD31^+$ endothelial cells from FA-iPSC-derived HAPCs (FA-HAPCs) was also reduced compared with that in the cFA-iPSC lines (Fig. 3E). The distribution of the cell cycle in FA-iPSC-derived KDR^+CD34^+ HAPCs was comparable to that of the complemented counterparts (supplemental online Fig. 6). We also confirmed that KDR^+CD34^+ HAPCs were not apoptotic (supplemental online Fig. 7). Although the expression level of p53 reduced and varied among the FA- or cFA-iPSC lines (supplemental online Fig. 2B), the ability of these cells to undergo hematopoietic differentiation was dependent on the FANCA status but not on the p53 level, indicating that, at least in this study, the expression level of p53 has no obvious impact on the differentiation propensity of HAPCs. Taken together, these findings indicate that FA-HAPCs showed a defective propensity to differentiate toward both hematopoietic and endothelial lineages.

To further elucidate the mechanism underlying the defective hematopoietic differentiation, we next quantified the expression levels of critical transcription factors requird for hematopoietic differentiation in HAPCs [17–20]. HAPCs from FA-iPSC lines showed significant downregulation of these transcription factors (Fig. 4A–4D), indicating that the FA pathway might be involved in maintaining the transcriptional network critical for determining the differentiation propensity of HAPCs. We also compared the global expression profiles of HAPCs from FA- and cFA-iPSCs (supplemental online Fig. 8A, 8B). We identified that 227 genes were significantly upregulated and 396 genes were significantly downregulated in FA-HAPCs (supplemental online Fig. 8C; supplemental online Table 2). A gene ontology enrichment analysis revealed that genes associated with mesodermal differentiation, vascular formation, and hematopoiesis were extensively downregulated in FA-HAPCs (supplemental online Fig. 8D).

Conclusion

In summary, we successfully established FA-iPSCs from FA-A patients. We found that an early pathological phenotype was detected in HAPCs as a defective differentiation propensity into both hematopoietic and endothelial lineages. Interestingly, during hematopoiesis, the expression of FANCA and FANCC were specifically upregulated in KDR^+CD34^+ HAPCs (supplemental online Fig. 9), indicating the stage-specific requirement of these genes in HAPCs. Because the expression of hematopoietic and angiogenic genes was affected, FANCA may have an important role in regulating these genes in FA-HAPCs. Conducting a comprehensive analysis of patient-derived affected progenitors is not feasible without iPSC technology, which provides an unprecedented opportunity to gain further insight into the pathogenesis of BMF in patients with FA.

Acknowledgments

We thank M. Yamane and S. Benno for technical assistance, H. Watanabe for administrative assistance, and M. Yoshida and K. Isoda for performing the teratoma assay. Funding was provided by grants from the Ministry of Health, Labor, and Welfare to T.N.; a grant from the Ministry of Education, Culture, Sports, Science, and Technology (MEXT) to T.N.; grants from the Leading Project of MEXT to T.N.; a grant from the Funding Program for World-Leading Innovative Research and Development on Science and Technology (FIRST Program) of the Japan Society for the Promotion of Science (JSPS) to T.N.; grants from the JSPS to T.N. and M.K.S.; a grant-in-aid from the Ministry of Education, Culture, Sports, Science, and Technology of Japan (Grant 20591262) to M.Y.; the Program for Intractable Diseases Research Utilizing Disease-Specific Induced Pluripotent Stem (iPS) Cells from the Japan Science and Technology Agency (JST) to T.N.; the grant for Core Center for iPS Cell Research of Research Center Network for Realization of Regenerative Medicine from JST to T.N. and M.K.S.; and a Research Grant for Intractable Diseases (H-21-061) from the Japanese Ministry of Health, Labor, and Welfare to M.Y.

Author Contributions

N.M.S.: collection and/or assembly of data, data analysis and interpretation, and manuscript writing; A.N., C.O., N.A., and A.W.: collection and/or assembly of data, data analysis and interpretation; M.Y.: provision of study material or patients; A.H.: data analysis and interpretation; K.-I.W. and T.H.: provision of study material or patients; M.T.: data analysis and interpretation, provision of study material or patients, conception and design; T.N.: conception and design, data analysis and interpretation; M.K.S.: conception and design, collection and/or assembly of data, data analysis and interpretation, manuscript writing, final approval of manuscript.

Disclosure of Potential Conflicts of Interest

C.O. is an uncompensated employee of the Mitsubishi Space Software Co., Ltd., with which CiRA entered into an agreement of bioinformatics analysis service. The other authors indicated no potential conflicts of interest.

References

1 Deans AJ, West SC. DNA interstrand crosslink repair and cancer. Nat Rev Cancer 2011;11:467–480.

2 Kottemann MC, Smogorzewska A. Fanconi anaemia and the repair of Watson and Crick DNA crosslinks. Nature 2013;493:356–363.

3 Kim H, D'Andrea AD. Regulation of DNA cross-link repair by the Fanconi anemia/BRCA pathway. Genes Dev 2012;26:1393–1408.

4 Takata M, Yamamoto K, Matsushita N et al. The Fanconi anemia pathway promotes homologous recombination repair in DT40 cell line. Subcell Biochem 2006;40:295–311.

5 Ceccaldi R, Parmar K, Mouly E et al. Bone marrow failure in Fanconi anemia is triggered by an exacerbated p53/p21 DNA damage response that impairs hematopoietic stem and progenitor cells. Cell Stem Cell 2012;11:36–49.

6 Kamimae-Lanning AN, Goloviznina NA, Kurre P. Fetal origins of hematopoietic failure in a murine model of Fanconi anemia. Blood 2013;121:2008–2012.

7 Takahashi K, Tanabe K, Ohnuki M et al. Induction of pluripotent stem cells from adult human fibroblasts by defined factors. Cell 2007;131:861–872.

8 Zhu Z, Huangfu D. Human pluripotent stem cells: An emerging model in developmental biology. Development 2013;140:705–717.

9 Okita K, Matsumura Y, Sato Y et al. A more efficient method to generate integration-free human iPS cells. Nat Methods 2011;8:409–412.

10 Niwa A, Heike T, Umeda K et al. A novel serum-free monolayer culture for orderly hematopoietic differentiation of human pluripotent cells via mesodermal progenitors. PLoS ONE 2011;6:e22261.

11 Yanagimachi MD, Niwa A, Tanaka T et al. Robust and highly-efficient differentiation of functional monocytic cells from human pluripotent stem cells under serum- and feeder cell-free conditions. PLoS ONE 2013;8:e59243.

12 Seki T, Yuasa S, Oda M et al. Generation of induced pluripotent stem cells from human terminally differentiated circulating T cells. Cell Stem Cell 2010;7:11–14.

13 Raya A, Rodriguez-Piza I, Guenechea G et al. Disease-corrected haematopoietic progenitors from Fanconi anaemia induced pluripotent stem cells. Nature 2009;460:53–59.

14 Muller LU, Milsom MD, Harris CE et al. Overcoming reprogramming resistance of Fanconi anemia cells. Blood 2012;119:5449–5457.

15 Muller LU, Schlaeger TM, DeVine AL et al. Induced pluripotent stem cells as a tool for gaining new insights into Fanconi anemia. Cell Cycle 2012;11:2985–2990.

16 Yung SK, Tilgner K, Ledran MH et al. Brief report: Human pluripotent stem cell models of Fanconi anemia deficiency reveal an important role for Fanconi anemia proteins in cellular reprogramming and survival of hematopoietic progenitors. Stem Cells 2013;31:1022–1029.

17 Scott EW, Simon MC, Anastasi J et al. Requirement of transcription factor PU.1 in the development of multiple hematopoietic lineages. Science 1994;265:1573–1577.

18 Okuda T, van Deursen J, Hiebert SW et al. AML1, the target of multiple chromosomal translocations in human leukemia, is essential for normal fetal liver hematopoiesis. Cell 1996;84:321–330.

19 Shivdasani RA, Mayer EL, Orkin SH. Absence of blood formation in mice lacking the T-cell leukaemia oncoprotein tal-1/SCL. Nature 1995;373:432–434.

20 Tsai FY, Keller G, Kuo FC et al. An early haematopoietic defect in mice lacking the transcription factor GATA-2. Nature 1994;371:221–226.

See www.StemCellsTM.com for supporting information available online.

J Clin Immunol (2015) 35:512–516
DOI 10.1007/s10875-015-0165-1

BRIEF COMMUNICATION

Mosaicism of an *ELANE* Mutation in an Asymptomatic Mother in a Familial Case of Cyclic Neutropenia

Osamu Hirata[1] · Satoshi Okada[1] · Miyuki Tsumura[1] · Shuhei Karakawa[1] · Itaru Matsumura[2] · Yujiro Kimura[3] · Toshiro Maihara[4] · Shin'ichiro Yasunaga[5] · Yoshihiro Takihara[5] · Osamu Ohara[6] · Masao Kobayashi[1]

Received: 2 June 2014 / Accepted: 13 April 2015 / Published online: 26 April 2015

Abstract
Purpose To confirm and characterize mosaicism of the cyclic neutropenia (CyN)-related mutation in the *ELANE* gene identified in the asymptomatic mother of patients with CyN.
Methods We identified sibling cases with CyN due to a novel heterozygous splicing site mutation, IVS4 +5SD G>T, in the *ELANE* gene, resulting in an internal in-frame deletion of 30 nucleotides (corresponding to a ten amino acid deletion, V161–F170). The mutated allele was also detected in their asymptomatic mother but at low frequency. We measured the frequency of the mutant allele from peripheral blood leukocytes (PBLs) by subcloning, and confirmed the allelic frequency of mosaicism in various cell types by massively parallel DNA sequencing (MPS) analysis.
Results In the subcloning analysis, the mutant allele was identified in 21.36 % of PBLs from the asymptomatic mother, compared with 54.72 % of PBLs from the CyN patient. In the MPS analysis, the mutant allele was observed in approximately 30 % of mononuclear cells, $CD3^+$ T cells, $CD14^+$ monocytes and the buccal mucosa. Conversely, it was detected in low frequency in polymorphonuclear leukocytes (PLMLs) (3–4 %) and $CD16^+$ granulocytes (2–3 %).
Conclusions Mosaicism of the *ELANE* mutation has only previously been identified in one confirmed and one unconfirmed case of SCN. This is the first report of mosaicism of the *ELANE* mutation in a case of CyN. The MPS results suggest that this de novo mutation occurred during the two-cell stage of embryogenesis. PLMLs expressing the *ELANE* mutation were found to be actively undergoing apoptosis.

Keywords *ELANE* · cyclic neutropenia · mosaicism · severe congenital neutropenia

Electronic supplementary material The online version of this article (doi:10.1007/s10875-015-0165-1) contains supplementary material, which is available to authorized users.

✉ Masao Kobayashi
masak@hiroshima-u.ac.jp

[1] Department of Pediatrics, Hiroshima University Graduate School of Biomedical & Health Sciences, 1-2-3 Kasumi, Minami-ku, Hiroshima 734-8551, Japan

[2] Department of Hematology and Rheumatology, Kinki University Faculty of Medicine, Osaka, Japan

[3] Department of Pediatrics, Kyotominami Hospital, Kyoto, Japan

[4] Department of Pediatrics, Hyogo Prefectural Tsukaguchi Hospital, Hyogo, Japan

[5] Department of Stem Cell Biology, Research Institute for Radiation Biology and Medicine, Hiroshima, Japan

[6] Department of Technology Development, Kazusa DNA Research Institute, Chiba, Japan

Introduction

Cyclic neutropenia (CyN) is a rare congenital disorder characterized by regular oscillations of peripheral blood neutrophil counts, generally with 21-day periodicity. Low absolute neutrophil counts affect the body's ability to fight infection resulting in frequent bacterial infections, cutaneous infections, gingivitis, stomatitis and pneumonia in patients [1, 2]. Heterozygous mutations in *ELANE*, the gene encoding neutrophil elastase, have been identified in 80–100 % of patients with CyN [3–5]. *ELANE* heterozygosity has also been identified in 35–69 % of patients with severe congenital neutropenia (SCN) [6–11]. In this study, we identified a sibling case with CyN resulting from a novel heterozygous splice site mutation, IVS4 +5SD G>T, in *ELANE*. This mutation was inherited in

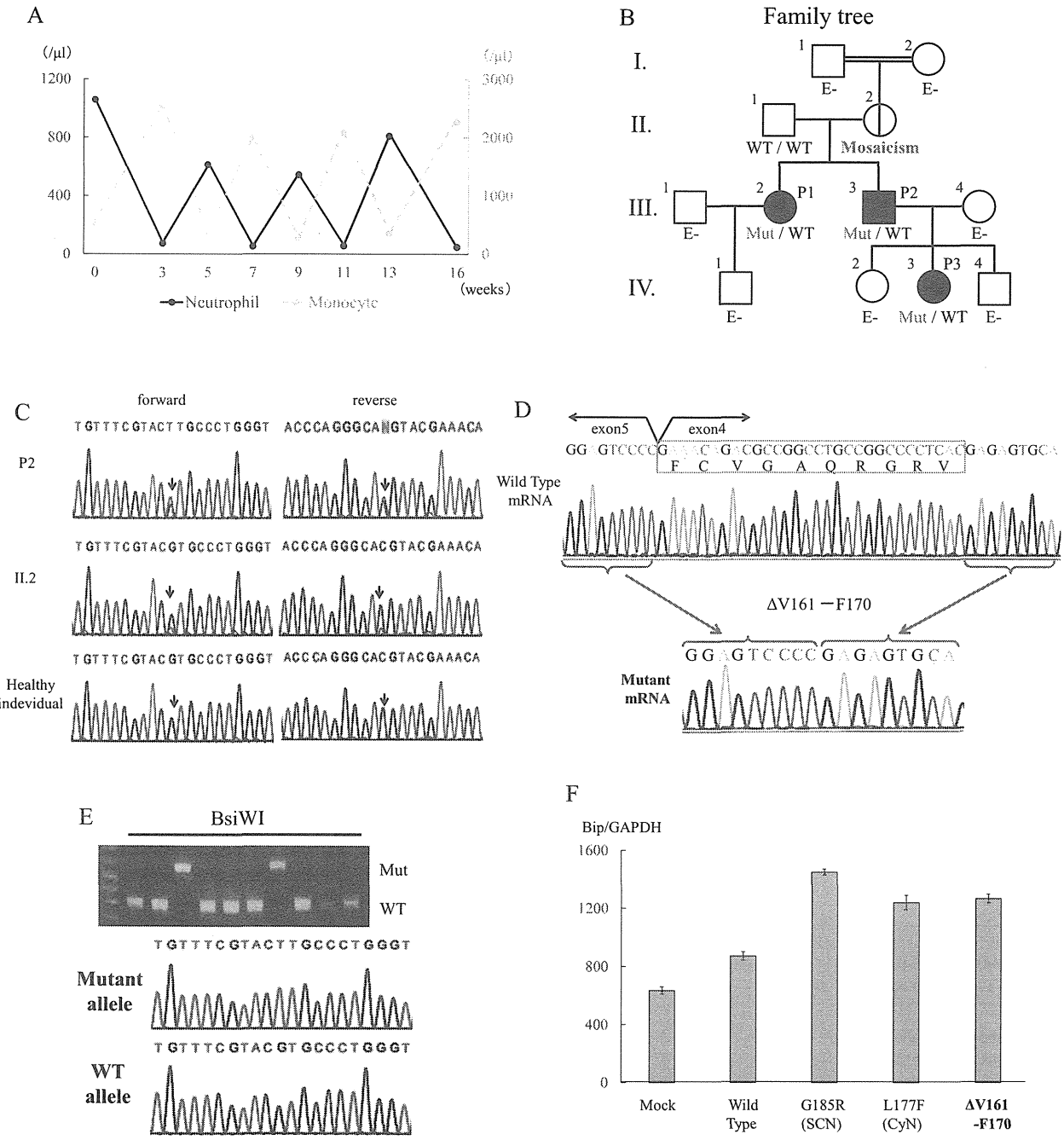

Fig. 1 Analysis of *ELANE* mutations in a familial case of cyclic neutropenia. **a** The time scourse of neutrophil counts in P3. Neutropenia of P3 recurred about every 3 weeks. Her absolute neutrophil count dropped to less than 200/μL during neutropenic periods. A reciprocal increase in blood monocytes occurred during the neutrophil nadir. **b, c** Identification and investigation of a heterozygous splice site mutation in the *ELANE* gene of CyN patients. P1, P2 and P3 presented intermittent neutropenia and were diagnosed with CyN. A heterozygous splice site mutation, IVS4 +5SD G>T, in the *ELANE* gene was identified in all three patients. The same mutation was also identified, but at low frequency, in their asymptomatic mother (II-2). **d** cDNA generated from the PBLs of P2 was subcloned and individual alleles were investigated. The splice site mutation led to an internal in-frame deletion of 30 nucleotides from the transcript and ten amino acid residues (V161–F170) from the protein. **e** The frequency of mutated alleles in PBLs was investigated by RFLP and sequence analysis. The *Bsi*WI restriction enzyme specifically restricts PCR products corresponding to the wild-type allele. The results of RFLP were consistent with those of sequence analysis. The frequency of the mutant allele was 21.36 % in the asymptomatic mother, compared with 54.72 % in P2. **f** Expression of mutant *ELANE* induces BiP mRNA expression in U2OS cells. Transient expression of *ELANE* mutants associated with SCN (G185R) or CyN (L177F and ΔV161–F170) induced higher levels of BiP mRNA expression compared with wild-type. BiP expression was normalized with respect to *GAPDH*. At least two independent experiments were performed

an autosomal dominant manner, apparently originating from their asymptomatic mother who carried mosaicism of the mutated allele. We purified various sample cell populations from the patients and examined the frequency of mutated alleles using massively parallel DNA sequencing (MPS) technology [12, 13]. Here, we describe the first case of mosaicism due to a CyN-related mutation in *ELANE*.

Case Report

The proband (P1: III-2) was a 32-year-old woman with a history of periodic recurrent bacterial infections and stomatitis. These infectious episodes were cured by treatment with antibiotics without the need for hospitalization. Neutropenia was detected at a routine periodic blood examination during pregnancy. After repeated observations of neutropenia, the woman was diagnosed with CyN at the age of 28. Sequence analysis of P1 showed a heterozygous splice site mutation in IVS4 +5SD G>T of the *ELANE* gene, resulting in the internal in-frame deletion of 30 nucleotides (a ten amino-acid deletion from V161 to F170). The same mutation was identified in her siblings, P2 (III-3) and P3 (IV-3). P2 had a history of periodic fever of unknown origin and stomatitis in childhood. These infectious episodes were treated with antibiotics and did not require hospitalization. P2 had only been hospitalized once to receive a tonsillectomy at the age of eight. P3 suffered from recurrent otitis media during periods of neutropenia. She was hospitalized twice with acute otitis media. Neutropenia (absolute neutrophil count<200/μL) of P3 recurred every 21 days and monocytes increased during neutropenic periods, reciprocally (Fig. 1a). Because an autosomal dominant identical *ELANE* mutation was observed in the older sister (P1) and younger brother (P2), one of their parents, despite being asymptomatic, was suspected to carry a germline mutation in *ELANE*. Genetic analysis revealed that P1's mother (II-2) had mosaicism of mutant *ELANE* alleles. Analysis of her medical history showed no obvious recurrent infectious episodes. Peripheral blood examinations of P1's mother were performed and repeated, and the results showed normal white blood cell counts (3,700 and 3,200/μL) and slightly decreased neutrophil counts (1,410 and 1,100/μL).

Informed consent was obtained from all patients, relatives and healthy adult controls who provided blood samples for this study. This study was approved by the Ethics Committee/Internal Review Board of Hiroshima University (Hiroshima, Japan). Detailed experimental methods are described in the Supplementary Methods section.

Results

Identification of a Mutation in the ELANE Gene and Maternal Mosaicism

Sequence analysis of all exons and flanking introns of the *ELANE* gene identified a novel heterozygous splice site mutation in IVS4 +5SD G>T in P1 (III-2), P2 (III-3) and P3 (IV-3) (Fig. 1b, c). We then synthesized cDNA from peripheral blood leukocytes (PBLs) from P2 and analyzed the effect of the mutation on splicing. This splice site mutation led to the internal in-frame deletion of 30 nucleotides from the transcript and ten amino acid residues (V161–F170) from the protein (Fig. 1d). A different nucleotide substitution at this position (IVS4 +5SD G>A), which disrupts splicing and results in the same 10-amino acid deletion, was identified previously in patients with CyN [4, 5]. Although the mutation was also identified in their asymptomatic mother (II-2) (Fig. 1b), it was detected at lower frequency. PCR products amplified from the patient's PBLs were subcloned and the frequency

Table 1 Mutant allele (IVS4 +5 G>T) frequencies detected by MPS analyses

Cell type	Experimental run	Total read	Mutant allele[a] frequencies (%)	
			Forward strand	Reverse strand
$CD14^+$ monocytes	1st	7023	35.7	35.1
	2nd	1676	25.8	27.3
$CD3^+$ T cells	1st	6701	32.2	30.9
	2nd	1596	30.1	30.9
MNCs	1st	5815	34.1	33.1
	2nd	1569	24.8	28.9
PMNLs	1st	6593	4.3	4.5
	2nd	1607	4.3	3.1
Buccal mucosa	1st	6210	30.3	30.3
$CD16^+$ granulocytes	2nd	1582	3.8	2.2

[a] All the mutant alleles exhibited *P*-values<10^{-24} obtained from the error map generated from wild-type alleles (about 4800 total reads) [12]

of the mutant allele was analyzed using the restriction fragment length polymorphism (RFLP) method (Fig 1e). Analysis of the first ten clones confirmed concordance between the results obtained with sequencing and RFLP analysis (Fig. 1e). The mutant allele was identified in 22 of the 103 clones (21.36 %) from the PBLs of the asymptomatic mother, compared with 58 of the 106 clones (54.72 %) from the PBLs of P2. These results suggested that the asymptomatic mother may exhibit mosaicism of the CyN-related *ELANE* mutation.

Investigation of Mosaicism of the CyN-Related Mutation in the ELANE Gene Using an MPS Approach

We further investigated the allelic frequency of mosaicism in the following cells: mononuclear cells (MNCs), polymorphonuclear leukocytes (PMNLs), $CD3^+$ T cells, $CD14^+$ monocytes, $CD16^+$ granulocytes and the buccal mucosa, using MPS technology [12]. Using this sequencing method, over 1500 alleles were analyzed for each of the individual cell populations and the frequencies of the mutant allele (IVS4 + 5SD G>A) are shown in Table 1. The mutant allele was observed at a frequency of approximately 30 % in MNCs, CD4+ T cells, CD14+ monocytes and buccal mucosa cells. Conversely, it was identified at low frequency in PMNLs (3–4 %) and CD16+ granulocytes (2–3 %), suggesting that the cells possessing the *ELANE* mutation undergo apoptosis early. The MPS data were comparable between two individual experiments and consistent with the results of the subcloning-based investigation.

Expression of Mutant ELANE in U2OS Cells Induces Endoplasmic Reticulum (ER) Stress

We investigated the expression of immunoglobulin heavy chain binding protein (BiP) mRNA, which is upregulated under conditions of ER stress. Human osteosarcoma (U2OS) cells transiently expressing SCN-related (G185R) or CyN-related (L177F and ΔV161–F170) *ELANE* induced higher levels of BiP compared with wild-type cells (Fig. 1f), with BiP expression being highest in cells transiently expressing the G185R *ELANE* mutant. Taken together, these findings confirmed that transient expression of *ELANE* mutants, regardless of whether the mutations were SCN- or CyN-related, induced ER stress in U2OS cells.

Discussion

We report the identification of a familial case of CyN resulting from a novel heterozygous mutation, IVS4 +5SD G>T, in the *ELANE* gene. This mutation was transmitted from an asymptomatic mother who exhibited mosaicism of the cells carrying the *ELANE* mutant allele. The MPS approach revealed that the majority of cells investigated, except for PMNLs and $CD16^+$ granulocytes, carried the mutant allele at a frequency of approximately 30 %. These results may suggest that the *de novo* mutation occurred during the two-cell stage in embryogenesis.

The clinical penetrance of *ELANE* mutations is known to be extremely high, thus we are generally able to observe strict familial segregation. The mosaicism of *ELANE* heterozygosity, which is responsible for SCN, has been previously identified in one confirmed and one unconfirmed case [14–16]. However, this is the first case of mosaicism due to a CyN-related mutation in the *ELANE* gene. In our study, the low frequency of the mutant allele in PMNLs and $CD16^+$ granulocytes from the asymptomatic mother was an interesting finding. This observation was consistent with a previous report of *ELANE* mosaicism in an asymptomatic father with SCN [14]. Mutations in the *ELANE* gene were reported to induce unfolded protein response-associated apoptosis at the promyelocyte stage [17–19]. BiP mRNA expression, a marker of ER stress, was significantly higher with our *ELANE* mutation (ΔV161–F170) than with the wild-type allele in transgenic lines. Thus, the discrepancy in the proportion of mutant alleles we observed in the asymptomatic mother might be explained by neutrophil-specific death due to apoptosis caused by *ELANE* mutations. Our case study indicates that like SCN-related mutations, CyN-related mutations can be asymptomatic in the case of mosaicism.

Acknowledgments This study was supported in part by Grants in Aid for Scientific Research from the Japan Society for the Promotion of Science [22591161 to M.K.], [25713039 to S.O.] and [80457241 to S.O.]. This study was also supported in part by Research on Measures for Intractable Diseases funding from the Japanese Ministry of Health, Labour and Welfare [H22-Nanchi-ippan-078 to M.K.]. Sequence analysis was supported by the Analysis Center of Life Science, Natural Science Center for Basic Research and Development, Hiroshima University (Hiroshima, Japan).

References

1. Dale DC, Hammond WP. Cyclic neutropenia: a clinical review. Blood Rev. 1988;2:178–85.
2. Palmer SE, Stephens K, Dale DC. Genetics, phenotype, and natural history of autosomal dominant cyclic hematopoiesis. Am J Med Genet. 1996;66:413–22.
3. Dale DC, Person RE, Bolyard AA, Aprikyan AG, Bos C, Bonilla MA, et al. Mutations in the gene encoding neutrophil elastase in congenital and cyclic neutropenia. Blood. 2000;96:2317–22.
4. Horwitz M, Benson KF, Person RE, Aprikyan AG, Dale DC. Mutations in ELA2, encoding neutrophil elastase, define a 21-day biological clock in cyclic haematopoiesis. Nat Genet. 1999;23:433–6.
5. Horwitz MS, Duan Z, Korkmaz B, Lee HH, Mealiffe ME, Salipante SJ. Neutrophil elastase in cyclic and severe congenital neutropenia. Blood. 2007;109:1817–24.
6. Bellanne-Chantelot C, Clauin S, Leblanc T, Cassinat B, Rodrigues-Lima F, Beaufils S, et al. Mutations in the ELA2 gene correlate with

more severe expression of neutropenia: a study of 81 patients from the French Neutropenia Register. Blood. 2004;103:4119–25.
7. Schäffer AA, Klein C. Genetic heterogeneity in severe congenital neutropenia: how many aberrant pathways can kill a neutrophil? Curr Opin Allergy Clin Immunol. 2007;7:481–94.
8. Ishikawa N, Okada S, Miki M, Shirao K, Kihara H, Tsumura M, et al. Neurodevelopmental abnormalities associated with severe congenital neutropenia due to the R86X mutation in the HAX1 gene. J Med Genet. 2008;45:802–7.
9. Sera Y, Kawaguchi H, Nakamura K, Sato T, Habara M, Okada S, et al. A comparison of the defective granulopoiesis in childhood cyclic neutropenia and in severe congenital neutropenia. Haematologica. 2005;90:1032–41.
10. Welte K, Zeidler C, Dale DC. Severe congenital neutropenia. Semin Hematol. 2006;43:189–95.
11. Xia J, Bolyard AA, Rodger E, Stein S, Aprikyan AA, Dale DC, et al. Prevalence of mutations in ELANE, GFI1, HAX1, SBDS, WAS and G6PC3 in patients with severe congenital neutropenia. Br J Haematol. 2009;147:535–42.
12. Izawa K, Hijikata A, Tanaka N, Kawai T, Saito MK, Goldbach-Mansky R, et al. Detection of base substitution-type somatic mosaicism of the NLRP3 gene with >99.9 % statistical confidence by massively parallel sequencing. DNA Res. 2012;19:143–52.
13. Flaherty P, Natsoulis G, Muralidharan O, Winters M, Buenrostro J, Bell J, et al. Ultrasensitive detection of rare mutations using next-generation targeted resequencing. Nucleic Acids Res. 2012;40:e2.
14. Ancliff PJ, Gale RE, Watts MJ, Liesner R, Hann IM, Strobel S, et al. Paternal mosaicism proves the pathogenic nature of mutations in neutrophil elastase in severe congenital neutropenia. Blood. 2002;100:707–9.
15. Benson KF, Horwitz M. Possibility of somatic mosaicism of ELA2 mutation overlooked in an asymptomatic father transmitting severe congenital neutropenia to two offspring. Br J Haematol. 2002;118:923. author reply923–4.
16. Germeshausen M, Schulze H, Ballmaier M, Zeidler C, Welte K. Mutations in the gene encoding neutrophil elastase (ELA2) are not sufficient to cause the phenotype of congenital neutropenia. Br J Haematol. 2001;115:222–4.
17. Grenda DS, Murakami M, Ghatak J, Xia J, Boxer LA, Dale D, et al. Mutations of the ELA2 gene found in patients with severe congenital neutropenia induce the unfolded protein response and cellular apoptosis. Blood. 2007;110:4179–87.
18. Klein C. Genetic defects in severe congenital neutropenia: emerging insights into life and death of human neutrophil granulocytes. Annu Rev Immunol. 2011;29:399–413.
19. Köllner I, Sodeik B, Schreek S, Heyn H, von Neuhoff N, Germeshausen M, et al. Mutations in neutrophil elastase causing congenital neutropenia lead to cytoplasmic protein accumulation and induction of the unfolded protein response. Blood. 2006;108:493–500.